

Adaptive Non-myopic Quantizer Design for Target Tracking in Wireless Sensor Networks

Sijia Liu*, Engin Masazade[†], Xiaojing Shen[‡], Pramod K. Varshney*

*Department of EECS, Syracuse University, Syracuse, NY, 13244, USA,
{sliu17, varshney}@syr.edu

[†]Department of Electrical and Electronics Engineering, Yeditepe University, Istanbul, 34755, Turkey, engin.masazade@yeditepe.edu.tr

[‡]Department of Mathematics, Sichuan University, Chengdu, Sichuan, 610064, China,
shenxj@scu.edu.cn

Abstract

In this paper, we investigate the problem of non-myopic (multi-step ahead) quantizer design for target tracking using a wireless sensor network. Adopting the alternative conditional posterior Cramér-Rao lower bound (A-CPCRLB) as an optimization metric, we theoretically show that this problem can be temporally decomposed over a certain time window. Based on sequential Monte-Carlo methods for tracking, i.e., particle filters, we design the local quantizer adaptively by solving a particle-based classical optimization problem which is well suited for using interior-point algorithm and easily embedded in the filtering process. Simulation results are provided to illustrate the effectiveness of our proposed approach for target tracking with quantized data by comparing its performance with some state-of-the-art methods.

I. INTRODUCTION

Wireless sensor networks (WSNs), consisting of a large number of spatially distributed sensors, have been used in a wide range of promising applications such as battlefield surveillance, environment and health monitoring. However, due to the limited resources on communication bandwidth and sensor power, it is desirable that only quantized data be transmitted from local sensor to a fusion center (FC). Particularly, target tracking with quantized data is an important problem which has been extensively studied in the literature [1]–[4]. In [1], the authors employed the static quantizer, which is first proposed

in [5] for estimating a static target location, to the tracking problem, where the optimal quantization thresholds are determined via maximizing the Fisher information about the signal amplitude contained in quantized data. Although this approach is robust and requires minimum prior information about the system, it doesn't yield the optimal solution for tracking scenario where the target state is random and dynamic. In [2], an adaptive binary quantizer is proposed to resolve the tracking problem by means of a particle filter. However, the scheme for adjusting local quantizers is heuristic and only corresponds to one bit per quantized observation. By taking into account the information content of measured data, two types of Monte Carlo-based adaptive quantizers are proposed in [3] and [4], respectively. With the use of variational filtering (VF), authors in [3] focus on optimizing the quantization level by maximizing the Fisher information matrix (FIM) under fixed and variable transmitting power. However, the proposed framework in [3] is limited to uniform quantizer. In [4], a general adaptive quantizer is presented in particle filtering-based tracking framework via minimizing direct conditional posterior Cramér-Rao lower bound (D-CPCRLB) [6]. Nevertheless, computing D-CPCRLB is expensive using the proposed person-by-person optimization (PBPO) method in [4] because the computational complexity highly relies on the size of predefined finite set of searching points. Considering the real-time requirement of adaptive quantizer design, it is important to seek more efficient algorithm to reduce the computation cost of optimization procedure.

Furthermore, for adaptive quantizers in [2]–[4], FC is required to feed the optimal quantizers back to local sensors at every time step (i.e., myopic/greedy strategy). As a consequence, the continual transmission might lead to data collision and channel congestion. In order to improve the transmission reliability, we are motivated to design the adaptive quantizers using the *non-myopic* (i.e., multi-steps ahead) strategy, which has drawn extensive attention on resource management such as adaptive compression [7] and sensor scheduling [8]. To the best of our knowledge, this is the first time the non-myopic strategy is studied in quantizer literature. Generally, the myopic design has lower computational cost than non-myopic design [9]. However, in this article, we will show that the non-myopic design is decomposable based on alternative conditional posterior Cramér-Rao lower bound (A-CPCRLB) [6]. Different from D-CPCRLB used in [4], A-CPCRLB yields a recursive FIM to support such decomposition in non-myopic quantizer design. Moreover, by virtue of the Monte-Carlo particles, the non-myopic quantizer design can be explicitly expressed as a classical optimization problem with differentiable objective and linear inequality constraints, and hence the optimal quantizers can be obtained via interior-point algorithm [10] that, we will show, is superior to the PBPO method of [4] in computation.

The rest of the paper is organized as follows. In Section II, we introduce the system model for target

tracking and formulate the A-CPCRLB based non-myopic quantizer design problem. In section III, we elaborate on the optimization procedure using Monte Carlo samples under particle filtering framework. To illustrate the effectiveness of our proposed approach, simulation results are presented in Section IV and finally Section V summarizes our work and discusses further research directions.

II. PROBLEM FORMULATION

In this paper, the task of the WSN is to monitor a single target moving in a two-dimensional Cartesian coordinate plane. At sampling instant t , the target state is defined by a 4×1 dimensional vector $\mathbf{x}_t = [x_t, y_t, \dot{x}_t, \dot{y}_t]$ and evolves according to the following equation

$$\mathbf{x}_{t+1} = \mathbf{F}\mathbf{x}_t + \mathbf{w}_t, \quad (1)$$

where x_t (or y_t) corresponds to the target location in the horizontal (or vertical) direction, \dot{x}_t (or \dot{y}_t) is the target velocity in the horizontal (or vertical) direction, \mathbf{F} models the state dynamics, and \mathbf{w}_t is white, Gaussian, zero-mean process noise with invertible covariance matrices \mathbf{Q} . Without loss of generality, we assume the state equation (1) satisfies a white noise acceleration model [1], where

$$\mathbf{F} = \begin{bmatrix} 1 & 0 & \Delta & 0 \\ 0 & 1 & 0 & \Delta \\ 0 & 0 & 1 & 0 \\ 0 & 0 & 0 & 1 \end{bmatrix}, \quad \mathbf{Q} = q \begin{bmatrix} \frac{\Delta^3}{3} & 0 & \frac{\Delta^2}{2} & 0 \\ 0 & \frac{\Delta^3}{3} & 0 & \frac{\Delta^2}{2} \\ \frac{\Delta^2}{2} & 0 & \Delta & 0 \\ 0 & \frac{\Delta^2}{2} & 0 & \Delta \end{bmatrix} \quad (2)$$

In (2), Δ and q denote the time interval between adjacent sensor measurements and the process noise parameter, respectively.

We further consider N sensors deployed in a region of interest (ROI) and each of them reports a noisy measurement, i.e.,

$$y_t^i = h_t^i(\mathbf{x}_t) + v_t^i, \quad (3)$$

for $i = 1, 2, \dots, N$, where y_t^i denotes a scalar observation from the i th sensor at time step t , v_t^i is white, Gaussian, zero-mean measurement noise with variance σ_v^2 , and function $h_t^i(\cdot)$ characterizes the observation model. As in [1], [4], the target is assumed to be an acoustic or an electromagnetic source that follows the isotropic attenuation model provided below

$$h_t^i(\mathbf{x}_t) = \sqrt{\frac{P_0}{1 + (d_t^i)^\nu}}. \quad (4)$$

In (4), P_0 denotes the signal power of the source, ν is the signal decay exponent, d_t^i is the distance between the target and the i th sensor, $d_t^i = \sqrt{(x_i - x_t)^2 + (y_i - y_t)^2}$, where (x_i, y_i) are the coordinates of the i th sensor.

A sensor measurement y_t^i is locally quantized before being sent to the fusion center (FC). Each sensor quantizes its measurement to M bits based on the following threshold quantizers

$$u_t^i = \begin{cases} 0 & -\infty < y_t^i \leq \gamma_{t,1}^i \\ \vdots & \vdots \\ L-1 & \gamma_{t,L-1}^i < y_t^i < +\infty \end{cases}, \quad (5)$$

where u_t^i denotes the quantized measurement of the i th sensor at time step t , $L = 2^M$, and the vector $\gamma_t^i := [\gamma_{t,1}^i, \dots, \gamma_{t,L-1}^i]^T$ corresponds to the quantization strategy of sensor i . For notational unification, let $\gamma_{t,0}^i = -\infty$ and $\gamma_{t,L}^i = \infty$. It is clear from (5) the probability of a particular quantization output l is

$$p(u_t^i = l | \mathbf{x}_t) = Q\left(\frac{\gamma_{t,l}^i - h_t^i(\mathbf{x}_t)}{\sigma_v}\right) - Q\left(\frac{\gamma_{t,l+1}^i - h_t^i(\mathbf{x}_t)}{\sigma_v}\right), \quad (6)$$

where $Q(\cdot)$ is the complementary distribution function of the standard Gaussian distribution.

Under the assumption of conditionally independent observations at local sensors, once the FC receives the quantized measurements at time step t , the observation likelihood function can be written as

$$p(\mathbf{u}_t | \mathbf{x}_t) = \prod_{i=1}^N p(u_t^i | \mathbf{x}_t), \quad (7)$$

where $\mathbf{u}_t = [u_t^1, u_t^2, \dots, u_t^N]^T$ denotes a collection of quantized measurements from N sensors. Note that the tracking performance can be affected by the observation likelihood $p(\mathbf{u}_t | \mathbf{x}_t)$, which is a function of quantization thresholds in (6). Therefore, it is important to develop efficient approaches to design optimal local quantizers at every time step.

A. Alternative conditional posterior Cramér-Rao lower bound (A-CPCRLB)

A conditional posterior Cramér-Rao lower bound (C-PCRLB) is proposed in [11] by incorporating a particular system state realization, which can provide a tighter error bound than conventional PCRLB in sequential Bayesian estimation. Nevertheless, computing C-PCRLB is expensive due to the auxiliary Fisher information matrix [11], which is not well suited for adaptive quantizer design. Instead, Zheng in [6] presented an alternative conditional PCRLB (A-CPCRLB), which is direct, more compact and computationally efficient. Thus, we adopt A-CPCRLB as the performance criterion to design optimal local quantizers in this work.

Let $\mathbf{x}_{0:t}$ and $\mathbf{u}_{1:t}$ denote the state vector and measurements up to time t . Then the conditional mean squared error of the state vector $\mathbf{x}_{0:t}$ is lower bounded by the inverse of conditional Fisher information matrix (C-FIM) as in [11]

$$E\{[\hat{\mathbf{x}}_{0:t+1} - \mathbf{x}_{0:t+1}][\hat{\mathbf{x}}_{0:t+1} - \mathbf{x}_{0:t+1}]^T | \mathbf{u}_{1:t}\} \geq J(\mathbf{x}_{0:t+1} | \mathbf{u}_{1:t})^{-1}. \quad (8)$$

Let $J(\mathbf{x}_{t+1} | \mathbf{u}_{1:t})$ be the matrix whose inverse equals to the lower-right corner submatrix of $J(\mathbf{x}_{0:t+1} | \mathbf{u}_{1:t})^{-1}$. Then the matrix $J(\mathbf{x}_{t+1} | \mathbf{u}_{1:t})$ will provide a lower bound on the mean square error (MSE) of estimating \mathbf{x}_{t+1} . As shown in [6], for the special case of linear state model with additive Gaussian noise, i.e., (1), the C-FIM $J(\mathbf{x}_{t+1} | \mathbf{u}_{1:t})$ can be computed as follows,

$$J_{t+1} \approx (Q + F J_t^{-1} F^T)^{-1} + E_{p_{t+1}^c} \{ -\Delta_{\mathbf{x}_{t+1}}^{\mathbf{x}_{t+1}} \ln p(\mathbf{u}_{t+1} | \mathbf{x}_{t+1}) \}, \quad (9)$$

where for notional simplicity we have used, and will henceforth continue to use, J_{t+1} instead of $J(\mathbf{x}_{t+1} | \mathbf{u}_{1:t})$, Δ is the second-order partial derivative, $p_{t+1}^c \triangleq p(\mathbf{x}_{t+1}, \mathbf{u}_{t+1} | \mathbf{u}_{1:t})$, F and Q corresponds to the state transmission matrix and process noise covariance in state model (1).

B. Non-myopic quantizer design

For non-myopic (multi-step ahead) quantizer design, we aim to seek optimal quantizers over a certain design window, $t+1 : t+T_w$, at time instant t , where T_w is the length of design window. It is clear from (7) and (9) that the value of C-FIM $J_{t+\eta}$ is dependant on quantization thresholds of local sensors at time $t+\eta$, denoted by $\gamma_{t+\eta} \triangleq [\gamma_{t+\eta}^1, \dots, \gamma_{t+\eta}^N]$, the previous C-FIM $J_{t+\eta-1}$, and the conditional distribution $p(\mathbf{x}_{t+\eta}, u_{t+\eta} | \mathbf{u}_{1:t+\eta-1})$, where $\eta \in \{1, 2, \dots, T_w\}$ and J_t is given as a prior information before designing. However, during the design window $t+1 : t+T_w$, $p(\mathbf{x}_{t+\eta}, u_{t+\eta} | \mathbf{u}_{1:t+\eta-1})$ cannot be achieved for $\eta > 1$ since the quantized measurements $u_{t:t+\eta-1}$ are not available at time t . Therefore, as in [8], the conditional distribution $p_{t+\eta}^c \triangleq p(\mathbf{x}_{t+\eta}, u_{t+\eta} | \mathbf{u}_{1:t+\eta-1})$ can be approximated by $p(\mathbf{x}_{t+\eta}, u_{t+\eta} | \mathbf{u}_{1:t})$, which is easily obtained in particle filter (see more details in Sec. III).

On the other hand, according to (9), it is easy to show that J_{t+T_w} is a function of $\{\gamma_{t+\eta}\}$ for $\eta = 1, 2, \dots, T_w$. Thus, in order to seek optimal quantization thresholds $\{\gamma_{t+\eta}\}_{\eta=1, \dots, T_w}$ for next T_w time steps, we pose the optimization problem as below via maximizing C-FIM at time $t+T_w$,

$$\begin{aligned} & \underset{\{\gamma_{t+\eta}\}_{\eta=1, \dots, T_w}}{\text{maximize}} && J_{t+T_w}(\gamma_{t+1}, \dots, \gamma_{t+T_w}) \\ & \text{subject to} && \gamma_{t+\eta,1}^i < \dots < \gamma_{t+\eta,L-1}^i \\ & && \text{for } \eta = 1, \dots, T_w \text{ and } i = 1, \dots, N \end{aligned} \quad (10)$$

where $\gamma_{t+\eta}$ is a $(L-1) \times N$ quantizer threshold matrix whose element $\gamma_{t+\eta,l}^i$ represents the l th threshold of sensor i at time $t + \eta$, L indicates the quantization levels, N is the number of sensors and T_w is the duration of time window. Moreover, the optimality for (10) is defined by positive semidefinite cone [10]. In other words, if $\{\gamma_{t+\eta}^*\}_{\eta=1,\dots,T_w}$ is the optimal solution of (10), we have $J_{t+Tw}(\gamma_{t+1}^*, \dots, \gamma_{t+Tw}^*) \succeq J_{t+Tw}(\gamma_{t+1}, \dots, \gamma_{t+Tw})$ (i.e., $J_{t+Tw}(\gamma_{t+1}^*, \dots, \gamma_{t+Tw}^*) - J_{t+Tw}(\gamma_{t+1}, \dots, \gamma_{t+Tw}) \succeq 0$) for arbitrary feasible $\{\gamma_{t+\eta}\}_{\eta=1,\dots,T_w}$, where $J \succeq 0$ denotes a matrix J is positive semidefinite. Then, in Proposition 1, we will show problem (10) can be further transformed to T_w sub-problems with scalar objective functions.

Proposition 1: If problem (10) has an optimal solution, solving (10) can be equivalently transformed to solve T_w subproblems, i.e.,

$$\begin{aligned} & \underset{\gamma_{t+\eta}}{\text{maximize}} \quad \text{tr} \left(E_{p_{t+\eta}^c} \left\{ -\Delta_{\mathbf{x}_{t+\eta}}^{\mathbf{x}_{t+\eta}} \ln p(\mathbf{u}_{t+\eta} | \mathbf{x}_{t+\eta}) \right\} \right) \\ & \text{subject to} \quad \gamma_{t+\eta,1}^i < \dots < \gamma_{t+\eta,L-1}^i, \quad i = 1, \dots, N \end{aligned} \quad (11)$$

for $\eta = 1, 2, \dots, T_w$, where $\text{tr}(\cdot)$ denotes the trace operator and $p_{t+\eta}^c \approx p(\mathbf{x}_{t+\eta}, u_{t+\eta} | \mathbf{u}_{1:t})$.

Proof:

According to (9), problem (10) can be decomposed into two subproblems

$$\begin{aligned} & \underset{\gamma_{t+Tw}}{\text{maximize}} \quad E_{p_{t+Tw}^c} \left\{ -\Delta_{\mathbf{x}_{t+Tw}}^{\mathbf{x}_{t+Tw}} \ln p(\mathbf{u}_{t+Tw} | \mathbf{x}_{t+Tw}) \right\} \\ & \text{subject to} \quad \gamma_{t+Tw,1}^i < \dots < \gamma_{t+Tw,L-1}^i, \quad i = 1, \dots, N \end{aligned} \quad (12)$$

and

$$\begin{aligned} & \underset{\{\gamma_{t+\eta}\}_{\eta=1,\dots,T_w-1}}{\text{maximize}} \quad (Q + F J_{t+Tw-1}^{-1} (\gamma_{t+1}, \dots, \gamma_{t+Tw-1}) F^T)^{-1} \\ & \text{subject to} \quad \gamma_{t+\eta,1}^i < \dots < \gamma_{t+\eta,L-1}^i \\ & \quad \text{for } \eta = 1, \dots, T_w - 1 \text{ and } i = 1, \dots, N \end{aligned} \quad (13)$$

where Q and F given in state equation (1). Since F is invertible, $Q \succ 0$ and $J_t \succ 0$ (i.e., Q and J_t are positive definite matrices), the problem (13) is equivalent to

$$\begin{aligned} & \underset{\{\gamma_{t+\eta}\}_{\eta=1,\dots,T_w-1}}{\text{maximize}} \quad J_{t+Tw-1}(\gamma_{t+1}, \dots, \gamma_{t+Tw-1}) \\ & \text{subject to} \quad \gamma_{t+\eta,1}^i < \dots < \gamma_{t+\eta,L-1}^i \\ & \quad \text{for } \eta = 1, \dots, T_w - 1 \text{ and } i = 1, \dots, N \end{aligned} \quad (14)$$

where we use the fact that for, any positive definite matrix, if $A \succeq B$ then $A^{-1} \preceq B^{-1}$.

After T_w recursive decomposition, (10) is equivalent to solve T_w problems given by

$$\begin{aligned} & \underset{\gamma_{t+\eta}}{\text{maximize}} \quad E_{p_{t+\eta}^c} \left\{ -\Delta_{\mathbf{x}_{t+\eta}}^{\mathbf{x}_{t+\eta}} \ln p(\mathbf{u}_{t+\eta} | \mathbf{x}_{t+\eta}) \right\} \\ & \text{subject to} \quad \gamma_{t+\eta,1}^i < \dots < \gamma_{t+\eta,L-1}^i, \quad i = 1, \dots, N \end{aligned} \quad (15)$$

Then by [12, Lemma 2.1], the problem (15) is equivalent to the problem (11). Now the proof is complete. \blacksquare

Remark 1: As $T_w = 1$, the non-myopic quantizer design in (10) becomes quantizers design in myopic (one-step ahead) way. However, designing quantizers myopically is different from solving the subproblem (11) over a certain time window due to the amount of available information. To be specific, at time $t + \eta$, the distribution $p_{t+\eta}^c$ in $J_{t+\eta}$ for myopic quantizer is conditioned on $\mathbf{u}_{1:t+\eta-1}$ rather than $\mathbf{u}_{1:t}$ in (11) for non-myopic quantizer.

Remark 2: Instead of A-CPCRLB, the conventional recursive PCRLB can be calculated offline [13] by using the target dynamic model (1) and sensor measurement model (3). In that case, it can be shown that the non-myopic quantizer design is equivalent to the myopic case based on the decomposition principle.

III. PARTICLE-BASED NON-MYOPIC QUANTIZER DESIGN

Sequential Monte Carlo methods such as particle filters have been widely used to evaluate the conditional PCRLB [11] and track the target with quantized data [1]. In this section, with the aid of sampling importance resampling (SIR) filter [14], we will show the problem of non-myopic quantizer design (11) can be solved as a classical optimization problem with differentiable objective and linear constraints.

Given the quantized sensor measurement $\mathbf{u}_{1:t}$, the goal of non-myopic quantizer design (10) is to determine optimal thresholds $\{\gamma_{t+\eta}\}_{\eta=1,\dots,T_w}$ for the next T_w time steps. **Proposition 1** has showed that problem (10) can be decomposed to solve T_w subproblems (11). At time step $t + \eta$, by substituting (7) into (11), the objective in (11) can be written as

$$\text{tr} \left(E_{p_{t+\eta}^c} \left\{ -\Delta_{\mathbf{x}_{t+\eta}}^{\mathbf{x}_{t+\eta}} \ln p(\mathbf{u}_{t+\eta} | \mathbf{x}_{t+\eta}) \right\} \right) = \sum_{i=1}^N \text{tr} \left(E_{p(\mathbf{x}_{t+\eta}, u_{t+\eta}^i | \mathbf{u}_{1:t})} \left\{ -\Delta_{\mathbf{x}_{t+\eta}}^{\mathbf{x}_{t+\eta}} \ln p(u_{t+\eta}^i | \mathbf{x}_{t+\eta}) \right\} \right),$$

where both the objective and constraints of (11) are separate over N sensors. Therefore, the problem (11) of seeking optimal quantizers for N sensors at time $t + \eta$ decomposes to subproblems

$$\begin{aligned} & \underset{\gamma_{t+\eta}^i}{\text{maximize}} \quad \psi(\gamma_{t+\eta}^i) \triangleq \text{tr} \left(E_{p(\mathbf{x}_{t+\eta}, u_{t+\eta}^i | \mathbf{u}_{1:t})} \left\{ -\Delta_{\mathbf{x}_{t+\eta}}^{\mathbf{x}_{t+\eta}} \ln p(u_{t+\eta}^i | \mathbf{x}_{t+\eta}) \right\} \right) \\ & \text{subject to} \quad \gamma_{t+\eta,1}^i < \dots < \gamma_{t+\eta,L-1}^i, \end{aligned} \tag{16}$$

which can be solved separately for $i = 1, 2, \dots, N$.

Using the fact that $u_{t+\eta}^i$, $\mathbf{x}_{t+\eta}$ and $\mathbf{u}_{1:t}$ form a Markov chain and the identity for standard Fisher information matrix [13]

$$E \left[\frac{\partial \ln p(u_{t+\eta}^i | \mathbf{x}_{t+\eta})}{\partial \mathbf{x}_{t,r}} \frac{\partial \ln p(u_{t+\eta}^i | \mathbf{x}_{t+\eta})}{\partial \mathbf{x}_{t,j}} \right] = -E \left[\frac{\partial^2 \ln p(u_{t+\eta}^i | \mathbf{x}_{t+\eta})}{\partial \mathbf{x}_{t,r} \partial \mathbf{x}_{t,j}} \right] \tag{17}$$

where $\mathbf{x}_{t,r}$ and $\mathbf{x}_{t,j}$ denote the r th entry and j th entry of state vector \mathbf{x}_t , the objective $\psi(\gamma_{t+\eta}^i)$ in (16) can be written as

$$\begin{aligned}\psi(\gamma_{t+\eta}^i) &= \sum_{r=1}^4 E_{p(\mathbf{x}_{t+\eta}|\mathbf{u}_{1:t})} \left\{ E_{p(u_{t+\eta}^i|\mathbf{x}_{t+\eta})} \left[\left(\frac{\partial \ln p(u_{t+\eta}^i|\mathbf{x}_{t+\eta})}{\partial x_{t+\eta,r}} \right)^2 \right] \right\} \\ &= \sum_{r=1}^4 \int_{\mathbf{x}_{t+\eta}} \left(\sum_{l=0}^{L-1} \left[\left(\frac{\partial \ln p(u_{t+\eta}^i = l|\mathbf{x}_{t+\eta})}{\partial x_{t+\eta,r}} \right)^2 \right] p(u_{t+\eta}^i = l|\mathbf{x}_{t+\eta}) \right) p(\mathbf{x}_{t+\eta}|\mathbf{u}_{1:t}) d\mathbf{x}_{t+\eta},\end{aligned}\quad (18)$$

where the likelihood $p(u_{t+\eta}^i = l|\mathbf{x}_{t+\eta})$ is given by (6) and

$$\begin{aligned}\frac{\partial \ln p(u_{t+\eta}^i = l|\mathbf{x}_{t+\eta})}{\partial \mathbf{x}_{t+\eta,r}} &= \frac{1}{p(u_{t+\eta}^i = l|\mathbf{x}_{t+\eta})} \frac{\partial p(u_{t+\eta}^i = l|\mathbf{x}_{t+\eta})}{\partial \mathbf{x}_{t+\eta,r}} \\ &= \frac{\frac{1}{\sigma_v} \frac{\partial h_{t+\eta}^i(\mathbf{x}_{t+\eta})}{\partial \mathbf{x}_{t+\eta,r}} \left[q\left(\frac{\gamma_{t+\eta,l}^i - h_{t+\eta}^i(\mathbf{x}_{t+\eta})}{\sigma_v}\right) - q\left(\frac{\gamma_{t+\eta,l+1}^i - h_{t+\eta}^i(\mathbf{x}_{t+\eta})}{\sigma_v}\right) \right]}{p(u_{t+\eta}^i = l|\mathbf{x}_{t+\eta})}.\end{aligned}\quad (19)$$

in which $q(\cdot)$ is the PDF of standard Gaussian distribution and $\frac{dQ(x)}{dx} = -q(x)$.

In SIR filter, we can approximate the posterior PDF $p(\mathbf{x}_t|\mathbf{u}_{1:t})$ by a set of particles $\{\mathbf{x}_t^s; s = 1, \dots, N_s\}$ with equal weights $1/N_s$ after the re-sampling process [14], where N_s is the total number of particles. Thus, the predicted PDF $p(\mathbf{x}_{t+\eta}|\mathbf{u}_{1:t})$ in (18) can be obtained by propagating particles \mathbf{x}_t^s after η steps using the state model (1). Then,

$$p(\mathbf{x}_{t+\eta}|\mathbf{u}_{1:t}) \approx \frac{1}{N_s} \sum_{s=1}^{N_s} \delta(\mathbf{x}_{t+\eta} - \mathbf{x}_{t+\eta}^s). \quad (20)$$

Substituting (6), (19) and (20) into (18), the optimization problem (16) can be written as

$$\begin{aligned}\underset{\gamma_{t+\eta}^i}{\text{maximize}} \quad & \psi(\gamma_{t+\eta}^i) \triangleq \sum_{l=0}^{L-1} f(\gamma_{t+\eta,l}^i, \gamma_{t+\eta,l+1}^i), \\ \text{subject to} \quad & \gamma_{t+\eta,1}^i < \gamma_{t+\eta,2}^i < \dots < \gamma_{t+\eta,L-1}^i\end{aligned}\quad (21)$$

where $\gamma_{t+\eta,0}^i = -\infty$, $\gamma_{t+\eta,L}^i = \infty$,

$$f(\gamma_{t+\eta,l}^i, \gamma_{t+\eta,l+1}^i) \triangleq \frac{1}{N_s \sigma_v^2} \sum_{s=1}^{N_s} \sum_{r=1}^4 h(\gamma_{t+\eta,l}^i, \gamma_{t+\eta,l+1}^i, \mathbf{x}_{t+\eta}^s, r), \quad (22)$$

and

$$h(\gamma_{t+\eta,l}^i, \gamma_{t+\eta,l+1}^i, \mathbf{x}_{t+\eta}^s, r) \triangleq \frac{\left(\frac{\partial h_{t+\eta}^i(\mathbf{x}_{t+\eta}^s)}{\partial \mathbf{x}_{t+\eta,r}} \right)^2 \left[q\left(\frac{\gamma_{t+\eta,l}^i - b_{t+\eta}^{i,s}}{\sigma_v}\right) - q\left(\frac{\gamma_{t+\eta,l+1}^i - b_{t+\eta}^{i,s}}{\sigma_v}\right) \right]^2}{Q\left(\frac{\gamma_{t+\eta,l}^i - b_{t+\eta}^{i,s}}{\sigma_v}\right) - Q\left(\frac{\gamma_{t+\eta,l+1}^i - b_{t+\eta}^{i,s}}{\sigma_v}\right)} \quad (23)$$

with $b_{t+\eta}^{i,s} \triangleq h_{t+\eta}^i(\mathbf{x}_{t+\eta}^s)$.

Moreover, it can be shown that the objective function in (21) is differentiable, and its first-order derivative is determined by the first-order derivative of $h(\gamma_{t+\eta,l}^i, \gamma_{t+\eta,l+1}^i, \mathbf{x}_{t+\eta}^s, r)$. Therefore, the interior-point algorithm [10] is well suited for solving problem (21) with differentiable objective and linear

constraint. In Algorithm 1, we summarize the procedure of Monte Carlo particle-based non-myopic quantizer design in the SIR filtering framework. A more detailed treatment of particle filtering can be found in a wide variety of publications such as [14].

Algorithm 1 Adaptive non-myopic quantizer design (10) based on SIR filter

- 1: At time t , begin with the updated particles \mathbf{x}_t^s and weights $w_t^s = N_s^{-1}$
 - 2: **for** $\eta = 1, \dots, T_w$ **do**
 - 3: Propagate particles by $\mathbf{x}_{t+1}^s = F\mathbf{x}_t^s + w_t$
 - 4: $p(x_{n+1}|u_{1:n_-}) = \frac{1}{N_s} \sum_{s=1}^{N_s} \delta(x_{n+1} - x_{n+1}^s)$
 - 5: Obtain optimal thresholds γ_{t+1}^i for N sensors by solving (21) for $i = 1, \dots, N$.
 - 6: **end for**
 - 7: Feed $\{\gamma_{t+\eta}\}_{\eta=1, \dots, T_w}$ back to local sensors and update particles by using the corresponding quantized measurement at $t+1, \dots, t+T_w$.
-

A. Binary Quantizer

For binary quantizer, i.e., $L = 2$, the optimization problem (21) becomes *unconstrained*, i.e.,

$$\underset{\gamma_{t+\eta,1}^i}{\text{maximize}} \quad f(\gamma_{t+\eta,0}^i, \gamma_{t+\eta,1}^i) + f(\gamma_{t+\eta,1}^i, \gamma_{t+\eta,2}^i) \quad (24)$$

where $\gamma_{t+\eta,0}^i = -\infty$ and $\gamma_{t+\eta,2}^i = \infty$. And the optimality condition for problem (24) is presented by the following proposition.

Proposition 2: The optimality condition of binary quantizer for sensor i at time $t+\eta$ can be expressed by a nonlinear equation

$$\begin{aligned} & \sum_{r=1}^4 \sum_{s=1}^{N_s} \left[\frac{\partial h_{t+\eta}^i(\mathbf{x}_{t+\eta}^s)}{\partial \mathbf{x}_{t+\eta,r}} \right]^2 \frac{2(\gamma_{t+\eta,1}^i - b_{t+\eta}^{i,s}) q^2(\frac{\gamma_{t+\eta,1}^i - b_{t+\eta}^{i,s}}{\sigma_v})}{Q(\frac{\gamma_{t+\eta,1}^i - b_{t+\eta}^{i,s}}{\sigma_v}) \left[1 - Q(\frac{\gamma_{t+\eta,1}^i - b_{t+\eta}^{i,s}}{\sigma_v}) \right]} \\ & + \sigma_v \sum_{r=1}^4 \sum_{s=1}^{N_s} \left[\frac{\partial h_{t+\eta}^i(\mathbf{x}_{t+\eta}^s)}{\partial \mathbf{x}_{t+\eta,r}} \right]^2 \frac{q^3(\frac{\gamma_{t+\eta,1}^i - b_{t+\eta}^{i,s}}{\sigma_v}) (2Q(\frac{\gamma_{t+\eta,1}^i - b_{t+\eta}^{i,s}}{\sigma_v}) - 1)}{Q^2(\frac{\gamma_{t+\eta,1}^i - b_{t+\eta}^{i,s}}{\sigma_v}) \left[1 - Q(\frac{\gamma_{t+\eta,1}^i - b_{t+\eta}^{i,s}}{\sigma_v}) \right]^2} = 0, \end{aligned} \quad (25)$$

where $\gamma_{t+\eta,1}^i$ represent the quantization threshold corresponding to the i th sensor at time $t+\eta$, $b_{t+\eta}^{i,s} \triangleq h_{t+\eta}^i(\mathbf{x}_{t+\eta}^s)$, and $\frac{\partial h_{t+\eta}^i(\mathbf{x}_{t+\eta}^s)}{\partial \mathbf{x}_{t+\eta,r}}$ is determined by the measurement model (4).

Proof: Eq. (25) can be directly obtained from the first-order derivative of $h(-\infty, \gamma_{t+\eta,1}^i, \mathbf{x}_{t+\eta}^s, r)$ and $h(\gamma_{t+\eta,1}^i, \infty, \mathbf{x}_{t+\eta}^s, r)$, where

$$\begin{aligned} h(\gamma_{t+\eta,0}^i, \gamma_{t+\eta,1}^i, \mathbf{x}_{t+\eta}^s, r) &= \left(\frac{\partial h_{t+\eta}^i(\mathbf{x}_{t+\eta}^s)}{\partial \mathbf{x}_{t+\eta,r}} \right)^2 \frac{q^2 \left(\frac{\gamma_{t+\eta,1}^i - b_{t+\eta}^{i,s}}{\sigma_v} \right)}{1 - Q\left(\frac{\gamma_{t+\eta,1}^i - b_{t+\eta}^{i,s}}{\sigma_v} \right)}, \\ h(\gamma_{t+\eta,1}^i, \gamma_{t+\eta,2}^i, \mathbf{x}_{t+\eta}^s, r) &= \left(\frac{\partial h_{t+\eta}^i(\mathbf{x}_{t+\eta}^s)}{\partial \mathbf{x}_{t+\eta,r}} \right)^2 \frac{q^2 \left(\frac{\gamma_{t+\eta,1}^i - b_{t+\eta}^{i,s}}{\sigma_v} \right)}{Q\left(\frac{\gamma_{t+\eta,1}^i - b_{t+\eta}^{i,s}}{\sigma_v} \right)}, \\ \frac{\partial h(\gamma_{t+\eta,0}^i, \gamma_{t+\eta,1}^i, \mathbf{x}_{t+\eta}^s, r)}{\partial \gamma_{t+\eta,1}^m} &= \left(\frac{\partial h_{t+\eta}^i(\mathbf{x}_{t+\eta}^s)}{\partial \mathbf{x}_{t+\eta,r}} \right)^2 \left[\frac{1}{\sigma_v^2} \frac{-2(\gamma_{t+\eta,1}^i - b_{t+\eta}^{i,s})q^2 \left(\frac{\gamma_{t+\eta,1}^i - b_{t+\eta}^{i,s}}{\sigma_v} \right)}{1 - Q\left(\frac{\gamma_{t+\eta,1}^i - b_{t+\eta}^{i,s}}{\sigma_v} \right)} - \frac{1}{\sigma_v} \frac{q^3 \left(\frac{\gamma_{t+\eta,1}^i - b_{t+\eta}^{i,s}}{\sigma_v} \right)}{\left(1 - Q\left(\frac{\gamma_{t+\eta,1}^i - b_{t+\eta}^{i,s}}{\sigma_v} \right) \right)^2} \right], \\ \frac{\partial h(\gamma_{t+\eta,1}^i, \gamma_{t+\eta,2}^i, \mathbf{x}_{t+\eta}^s, r)}{\partial \gamma_{t+\eta,1}^i} &= \left(\frac{\partial h_{t+\eta}^i(\mathbf{x}_{t+\eta}^s)}{\partial \mathbf{x}_{t+\eta,r}} \right)^2 \left[\frac{1}{\sigma_v^2} \frac{-2(\gamma_{t+\eta,1}^i - b_{t+\eta}^{i,s})q^2 \left(\frac{\gamma_{t+\eta,1}^i - b_{t+\eta}^{i,s}}{\sigma_v} \right)}{Q\left(\frac{\gamma_{t+\eta,1}^i - b_{t+\eta}^{i,s}}{\sigma_v} \right)} + \frac{1}{\sigma_v} \frac{q^3 \left(\frac{\gamma_{t+\eta,1}^i - b_{t+\eta}^{i,s}}{\sigma_v} \right)}{Q^2\left(\frac{\gamma_{t+\eta,1}^i - b_{t+\eta}^{i,s}}{\sigma_v} \right)} \right] \end{aligned}$$

■

To solve the nonlinear algebraic equation (25), a quasi-Newton method, provided by MATLAB's `fsolve` function, can be used in practice.

B. Identical Quantizer

In order to reduce the computation cost of optimization procedure, authors in [4] proposed to employ identical thresholds for all of local sensors. But it is clear from (21) that based on the power attenuation model (4) the local quantizer design much relies on the sensor locations and predicted measurements $h_{t+\eta}^i(\mathbf{x}_{t+\eta}^s)$. Therefore, the identical thresholds results in performance degradation [4]. Further, we consider a linear measurement model $y_t^i = \mathbf{h}_t^i \mathbf{x}_t + v_t^i$ for sensor i at time t , where \mathbf{h}_t^i is a observation vector to characterize the scalar measurement. If $\mathbf{h}_t^1 = \dots = \mathbf{h}_t^M$ (e.g., the mean estimation problem in [15]), it can be shown that the quantizer design, i.e., problem (21), yields identical quantization thresholds for M sensors at every time instant.

IV. SIMULATION RESULTS

In our simulations, we consider $N = 9$ sensors are grid deployed in a 20×20 m^2 surveillance area. For target motion in (1), we select sampling interval $\Delta = 0.5$ seconds and process noise parameter $q \in \{0.1, 2.5 \times 10^{-3}\}$, where the value of q indicates the relative uncertainty on target trajectory. The initial state distribution of the target is assume to be Gaussian with mean $\mu_0 = [-8.8, -8.8, 1.8, 1.8]$ and covariance $\Sigma_0 = \text{diag}[\sigma_0^2, \sigma_0^2, 0.01, 0.01]$ with $3\sigma_0 = 2$. We perform target tracking over 10 seconds, i.e., 20 time steps, see Fig. 1 for an example of target trajectories. The sensor measurements are obtained

from (3), where $P_0 = 1000$, $\nu = 2$ and sensor observation noise $\sigma_v = 0.1$. Without loss of generality, we assume each sensor quantizes its measurement with $M \leq 3$ bits. It is further assumed that the fusion center has perfect information about the target dynamical model as well as the noise statistics. The number of particles used in particle filter is 1000. And the tracking performance is evaluated via mean square error (MSE), which is averaged over 100 Monte-Carlo trials.

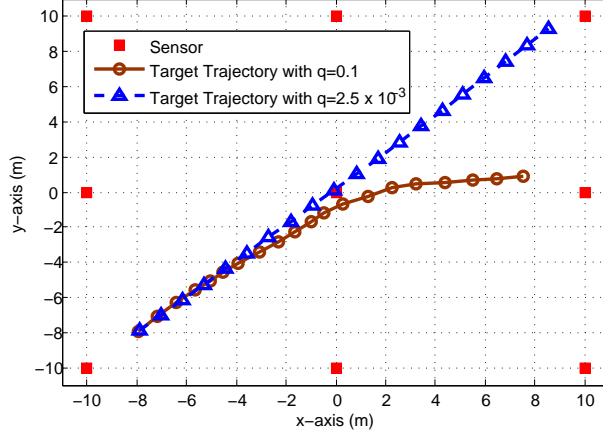


Fig. 1: Target trajectories as process noise parameter $q = 0.1$ and 2.5×10^{-3} in a WSN of $N = 9$ sensors

As in [2]–[4], designing non-myopic quantizer based on A-CPCRLB is a online process, thus, it is important to reduce the computation time such that the optimal quantizer can be solved before local sensors quantize their analog observations. According to the optimization problem (21), one straightforward idea is to express the predicted distribution $p(\mathbf{x}_{t+\eta}|\mathbf{u}_{1:t})$ with an decreasing number of particles as quantizer design. Therefore, in Fig. 2-(a), for different quantization bits, we evaluate the computation time of solving problem (21) by using the `etime` function of MATLAB versus the number of Monte-Carlo particles that varies over $\{1, 50, 200, 1000\}$. As we can see, the computation time goes up as the number of particles to approximate $p(\mathbf{x}_{t+\eta}|\mathbf{u}_{1:t})$ increases. And for multi-bits quantizer (e.g., $M = 3$), solving (21) with a large number of particles becomes impractical. Therefore, it is worthwhile to investigate how the tracking performance degrades while using less number of particles to approximate $p(\mathbf{x}_{t+\eta}|\mathbf{u}_{1:t})$ in quantizer design. In Fig. 2-(b), we demonstrate the tracking performance of 1-bit myopic quantizer (i.e., the length of design window $T_w = 1$) with process noise parameter $q = 0.1$ as the number of particles varies in $\{1, 50, 200, 1000\}$. For comparison, the estimation performance obtained from analog observation/data (AD) is also plotted. As we can see, the MSE cannot be improved much when 200 or 1000 particles used compared to 50 particles, which yield a better tradeoff between computation cost and

estimation performance. Thus, in the following simulations, we employ 50 particles for quantizer design, but in the part of target tracking, we keep 1000 particles to update the target state.

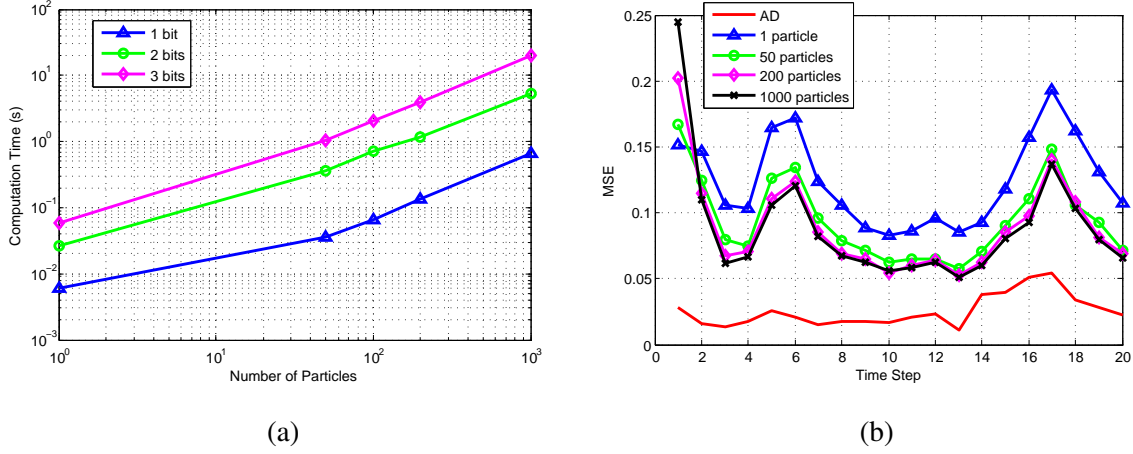


Fig. 2: Computation cost and tracking performance against the number of particles (a) Computation time for $M = 1, 2$, and 3 (b) MSE for 1-bit myopic quantizer with $q = 0.1$

In Fig. 3, we demonstrate the MSE at each time step of tracking averaged over 100 Monte-Carlo trials by using 2-bits non-myopic quantizer with the length of time design window $T_w \in \{1, 5, 10, 20\}$, where the non-myopic design with $T_w = 1$ is equivalent to the myopic design, and the non-myopic quantizer with $T_w = 20$ becomes offline since the corresponding A-CPCRLB can be calculated offline. For comparison, we also present the tracking performance of analog observation and quantized data based on the offline Fisher information heuristic quantizer (FIHQ) proposed in [5]. As the process noise parameter $q = 0.1$, Fig. 3-(a) shows that the estimation performance is improved as the size of design window decreases. That is because for $q = 0.1$ the target trajectory has relatively large uncertainty so that the accuracy of estimation benefits from quantizer design using more online information (i.e., sensors measurements), which corresponds to a small design window. For $q = 2.5 \times 10^{-3}$, Fig. 3-(b) shows that the MSE gets close for different sizes of design window since the process noise is relatively small and the target trajectory is almost deterministic/predictable such that the non-myopic quantizer only based on predicted particles with $T_w = 20$ can yield similar MSE performance compared to the myopic design with $T_w = 1$. Furthermore, in Fig. 3-(b), it can be seen the tracking performance of using our proposed offline quantizer (i.e., $T_w = 20$) significantly outperforms the performance of FIHQ due to the uniform assumption for target and sensors in [5]. As the process noise increases, i.e., $q = 0.1$ in Fig. 3-(a), the MSE of our proposed offline quantizer (i.e., $T_w = 20$) approaches to the MSE of FIHQ at the final time

step since the accumulative error goes up as time increases when the target trajectory has relatively large uncertainty.

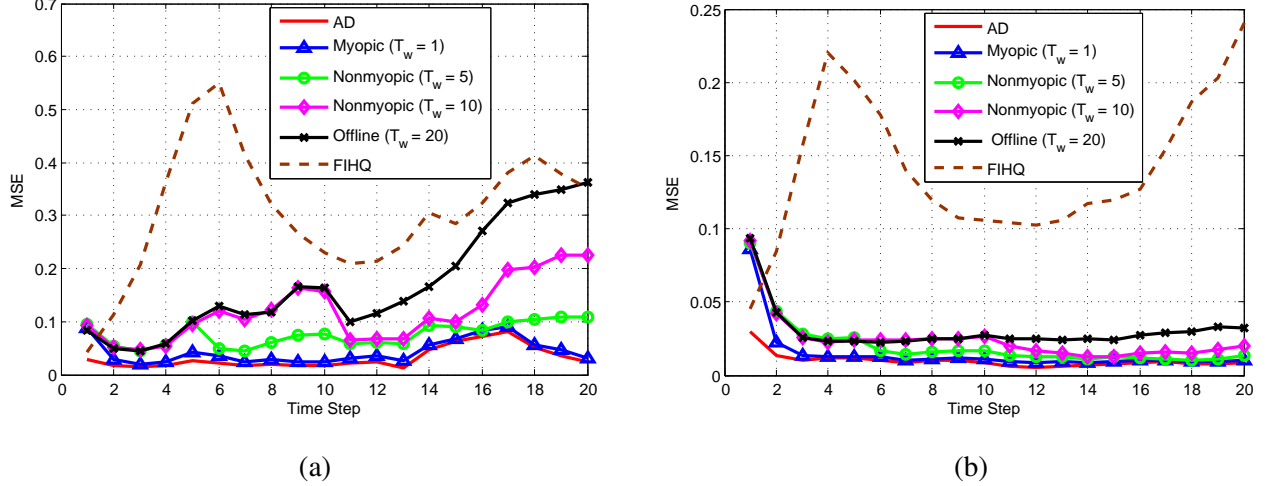


Fig. 3: Tracking performance of non-myopic quantizer with different sizes of design (a) $q = 0.1$ and $\sigma_v = 0.1$ (b) $q = 2.5 \times 10^{-3}$ and $\sigma_v = 0.1$

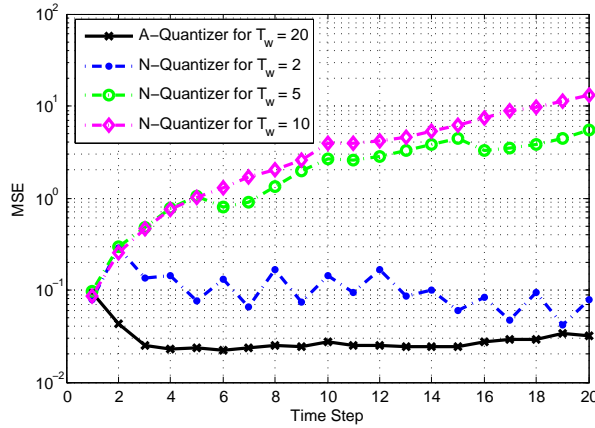
Further, we compare our approach for myopic quantizer design (i.e., $T_w = 1$) with the adaptive local quantizer proposed in [4]. From the perspective of MSE, the two methods almost yield same estimation performance. Here, we omit the simulation results for the sake of brevity. However, the adaptive quantizer proposed in [4] takes higher computational cost. Table I compares the execution times of the two methods for different number of bits, i.e., $M = 1, 2$ and 3 . As we can see, on a 3 GHz computer, our method requires less time than [4], since the optimal thresholds in [4] are obtained via a person-by-person optimization (PBPO) procedure, whose computational complexity mainly depends on the scale of predefined search set and the number of sensors. However, in our approach, the quantizer design can be decomposed to subproblem for each sensor at every time instant, and we employ interior-point algorithm in optimization which yields the gradient as the searching direction instead of blind search in PBPO. Note that in Table I, the execution time of using 3 bits is less than 2 bits for the method of [4], since the number of possible combinations for threshold values corresponding to $M = 3$ bits in a predefined search set, which, for example, contains $K = 8$ discrete points and thus has $\binom{8}{7}$ combinations, is less than the case for $M = 2$ bits.

In Fig. 4, we present the MSE of temporally identical quantizer (I-Quantizer), which refers to designing quantizers only for the next time step and then using the same quantizers in the entire window. For

TABLE I: Execution times in seconds for our proposed approach and method in [4]

	Our proposed method	Method in [4]
$M = 1$	0.0361	0.6205
$M = 2$	0.3603	6.2682
$M = 3$	1.0342	2.0026

comparison, the MSE of nonidentical quantizer (N-Quantizer) with $T_w = 20$ is also plotted. Simulation results show that the tracking performance of I-Quantizer is worse than the N-Quantizer even with a small window size (i.e., $T_w = 2$). That is because in tracking scenario the target state is random and dynamic, which leads to a large innovation error by using identical quantizer in time, even though the identical design can save energy and computation cost.

Fig. 4: MSE performances of 2-bits quantizer as $q = 2.5 \times 10^{-3}$

V. CONCLUSION

In this paper, we consider a problem of target tracking with quantized data, where the optimal local quantizers are determined using the non-myopic strategy, i.e, for next multiple time steps, which is beneficial to reducing the communication frequency between fusion center and local sensors. Using the alternative conditional posterior Cramér-Rao lower bound (A-CPCRLB), we theoretically show the problem of non-myopic quantizer can be decomposed temporally over a design window, and thus yield the same computational complexity as the myopic quantizer in [3], [4]. Further, based on particle filters

in tracking, a Monte-Carlo based quantizer design problem can be formulated and solved via the interior-point algorithm, which yields efficient and reliable performance shown by simulation results. In future, we will extend the proposed quantizer design in target tracking to many other contexts such as diffusive source localization and field estimation. We will also consider a unified non-myopic optimization framework by incorporating the resource management problems such as sensor selection and bandwidth allocation.

REFERENCES

- [1] E. Masazade, Ruixin Niu, and P.K. Varshney, “Dynamic bit allocation for object tracking in wireless sensor networks,” *IEEE Transactions on Signal Processing*, vol. 60, no. 10, pp. 5048–5063, oct. 2012.
- [2] M. Vemula, M.F. Bugallo, and P.M. Djuric, “Particle filtering-based target tracking in binary sensor networks using adaptive thresholds,” in *IEEE International Workshop on Computational Advances in Multi-Sensor Adaptive Processing*, dec. 2007, pp. 17 –20.
- [3] Majdi Mansouri, Ouachani Ilham, Hichem Snoussi, and Cédric Richard, “Adaptive quantized target tracking in wireless sensor networks,” *Wireless Networks*, vol. 17, no. 7, pp. 1625–1639, Oct. 2011.
- [4] O. Ozdemir, Ruixin Niu, and P.K. Varshney, “Adaptive local quantizer design for tracking in a wireless sensor network,” in *42nd Asilomar Conference on Signals, Systems and Computers*, oct. 2008, pp. 1202 –1206.
- [5] R. Niu and P. K. Varshney, “Target location estimation in sensor networks with quantized data,” *IEEE Transactions on Signal Processing*, vol. 54, no. 12, pp. 4519 –4528, Dec. 2006.
- [6] Yujiao Zheng, O. Ozdemir, Ruixin Niu, and P.K. Varshney, “New conditional posterior cramer-rao lower bounds for nonlinear sequential bayesian estimation,” *IEEE Transactions on Signal Processing*, vol. 60, no. 10, pp. 5549 –5556, oct. 2012.
- [7] E. Liu, Edwin K. P. Chong, and Louis L. Scharf, “Greedy adaptive compression in signal-plus-noise models,” *submitted to IEEE Transactions on Information Theory*, 2012, .
- [8] Engin Masazade, Ruixin Niu, and Pramod K. Varshney, “An approximate dynamic programming based non-myopic sensor selection method for target tracking,” in *46th Annual Conference on Information Sciences and Systems (CISS)*, march 2012, pp. 1 –6.
- [9] Amit S. Chhetri, Darryl Morrell, and Antonia Papandreou-Suppappola, “Nonmyopic sensor scheduling and its efficient implementation for target tracking applications,” *EURASIP J. Appl. Signal Process.*, vol. 2006, pp. 9–9, Jan. 2006.
- [10] S. Boyd, *Convex Optimization*, Cambridge University Press, Cambridge, 2004.
- [11] Long Zuo, Ruixin Niu, and P.K. Varshney, “Conditional posterior cramer rao lower bounds for nonlinear sequential bayesian estimation,” *IEEE Transactions on Signal Processing*, vol. 59, no. 1, pp. 1 –14, jan. 2011.
- [12] X. Shen and P. K. Varshney, “Sensor selection based on generalized information gain for target tracking in large sensor networks,” *Arxiv preprint <http://arxiv.org/abs/1302.1616>*, 2013.
- [13] H. L. Van Trees and K. L. Bell, *Bayesian Bounds for Parameter Estimation and Nonlinear Filtering Tracking*, Wiley-IEEE press, 2007.
- [14] M.S. Arulampalam, S. Maskell, N. Gordon, and T. Clapp, “A tutorial on particle filters for online nonlinear/non-gaussian bayesian tracking,” *IEEE Transactions on Signal Processing*, vol. 50, no. 2, pp. 174 –188, feb 2002.
- [15] A. Vempaty, B. Chen, and P. Varshney, “Optimal quantizers for bayesian distributed estimation,” *submitted to IEEE International Conference on Acoustics, Speech and Signal Processing (ICASSP’13)*, 2013.